Available online at www.synsint.com

Synthesis and Sintering

ISSN 2564-0186 (Print), ISSN 2564-0194 (Online)

Research article

Design and finite element analysis of a bio-inspired cellular airfoil for selective laser melting

Ata Khabaz-Aghdam *, Elisee Abu Mulamba Tshibeng, Omar Wambele Nsimba

Department of Aeronautical Engineering, Faculty of Aviation and Space Sciences, University of Kyrenia, Kyrenia, Mersin 10, Turkey

ABSTRACT

The development of lightweight aerospace structures with high structural efficiency has increased interest in bio-inspired cellular architectures and additive manufacturing. In this study, a bio-inspired cellular airfoil developed as a candidate architecture for future fabrication by selective laser melting (SLM) is proposed and systematically investigated using finite element analysis. The internal architecture, inspired by the hierarchical structural characteristics of banana stems and spiral shells, was generated through a parametric methodology and integrated into NACA0010 and NACA2412 airfoil profiles. Eighteen configurations were created by varying the position factor (K_1) and scaling factor (K_2), and their mechanical responses were evaluated under bending using an elastic–perfectly plastic material model. The effects of the geometric parameters on load–displacement response, bending stiffness, von Mises stress distribution, and first-yield load were examined. The NACA2412 configurations exhibited bending stiffness values of 84.0–99.9 kN/mm, approximately twice those of the NACA0010 designs (41.2–48.0 kN/mm). The highest stiffness of 99.9 kN/mm was obtained for the NACA2412 configuration with K_1=0.5 and K_2=0.5; however, this design developed a maximum von Mises stress of 360 MPa and an estimated first-yield load of 16.0 kN. In contrast, the NACA2412 configuration with K_1=0.75 and K_2=0.5 achieved a bending stiffness of 90.6 kN/mm, a lower peak stress of 276.7 MPa, and the highest estimated first-yield load of 18.8 kN. These results demonstrate that maximizing structural stiffness alone does not necessarily provide the optimum cellular architecture and that the combined control of cellular size and internal member positioning is essential for balancing global stiffness and local stress concentration. The proposed parametric design framework provides a practical approach for developing structurally efficient bio-inspired cellular airfoils suitable for SLM-based aerospace applications.

KEYWORDS

Bio-inspired design
Selective laser melting
Laser powder bed fusion
Cellular airfoil
Finite element analysis
Lightweight structures

OPEN ACCESS

1. Introduction

The continuous demand for improved fuel efficiency, reduced environmental impact, and enhanced structural performance has made lightweight design a central objective in modern aerospace engineering. Reducing structural mass while maintaining adequate stiffness, strength, and damage resistance remains a major challenge in aircraft structural design. In this context, architected cellular and lattice materials have attracted considerable attention because their mechanical response can be tailored through the geometry, size, and spatial arrangement of their internal architecture [1–3]. Unlike conventional monolithic structures, these materials provide additional geometric design variables that enable stiffness, load transfer, and local

* Corresponding author. *E-mail address:* ata.khabazaghdam@kyrenia.edu.tr (A. Khabaz-Aghdam)

Received 10 May 2026; Received in revised form 27 June 2026; Accepted 27 June 2026.

https://doi.org/10.53063/synsint.2026.62340

mechanical response to be controlled independently of the constituent material. Recent developments in additive manufacturing (AM) have further expanded the application of such architectures by enabling the fabrication of complex internal geometries that are difficult or impractical to produce using conventional manufacturing methods [1, 3].

Nature provides numerous examples of lightweight cellular structures in which structural efficiency is achieved through hierarchical and spatially varying architectures. Biological systems such as bone, wood, plant tissues, and shells combine geometric hierarchy with non-uniform material distribution to satisfy multiple functional and mechanical requirements [4–7]. These characteristics have motivated the development of bio-inspired architected materials in which selected geometric principles of natural systems are abstracted and transferred to engineering structures. The increasing accessibility of AM has particularly accelerated this approach because complex biomimetic geometries can now be translated directly from computational models into physical components [4, 6, 7].

Among plant-based biological systems, the banana pseudostem exhibits a hierarchical cellular organization that has recently attracted attention as a source of structural inspiration. Saputro et al. [8] developed three-dimensional printed banana-pseudostem-like structures and demonstrated the feasibility of translating their cellular organization into engineered architectures. Spiral shell geometries have similarly been investigated as adaptable natural structures. Chen et al. [9] used parametric analysis to examine the geometric and structural characteristics of spiraled shells, demonstrating the potential of mathematical abstraction for transferring naturally occurring geometric patterns to engineering design. Shell-inspired cellular and lattice architectures have also been explored in additively manufactured structures, where spiral-like arrangements provide an alternative to conventional periodic unit-cell designs [10]. Based on these natural concepts, the present design abstracts the hierarchical cellular organization of the banana pseudostem and the progressive spiral-like arrangement observed in shell structures to develop the proposed internal airfoil architecture, as illustrated in Fig. 1. These studies suggest that natural geometries need not be directly replicated; rather, their characteristic hierarchical or spatial organization can be abstracted to generate new structural concepts.

The realization of complex bio-inspired cellular architectures is closely linked to advances in metal additive manufacturing. Selective laser melting (SLM), also referred to within the broader class of laser powder bed fusion processes, enables metallic components with interconnected cellular and lattice geometries to be manufactured directly from digital models. This capability has made SLM particularly attractive for lightweight aerospace structures and architected materials [1, 3, 7]. AlSi10Mg is widely investigated for SLM-based cellular structures because of its low density and suitability for laser-based processing. Li et al. [11] experimentally investigated SLM-fabricated AlSi10Mg diamond lattices and demonstrated that the geometry and volume fraction of the cellular architecture strongly affect their mechanical response. Other studies have shown that local geometric features, strut orientation, feature size, and process-induced defects can significantly influence the mechanical performance of SLM cellular structures [12–15]. Therefore, the structural design of an additively manufactured cellular component should consider not only the constituent material but also the arrangement and connectivity of its internal members.

The potential of cellular architectures has also been investigated for aircraft wing structures. Khan et al. [16] studied lattice-infilled wing designs as alternatives to conventional spar–rib architectures and demonstrated that the selection of the internal lattice topology strongly influences structural deformation, stress distribution, and weight reduction. Bio-inspired concepts have also been introduced into aircraft wing design; for example, bird-bone-like internal structures have been investigated as non-conventional lightweight wing architectures [17].

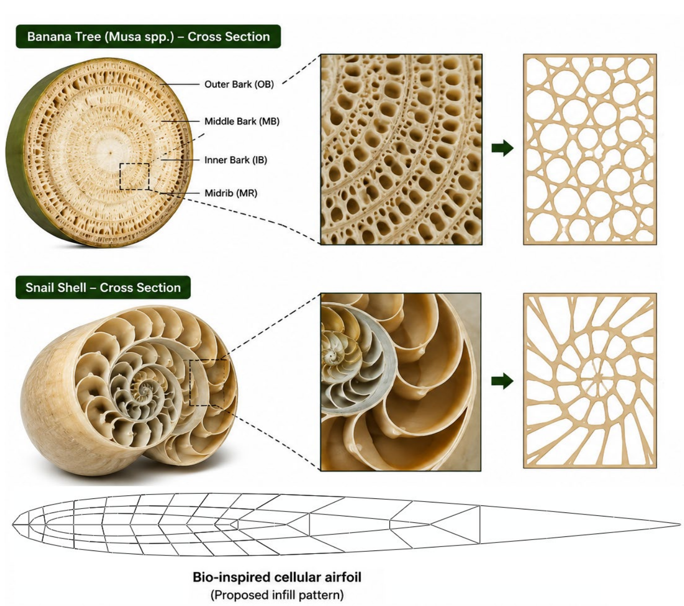

Fig. 1. Bio-inspired design concept illustrating the natural inspiration from the banana stem cross-section and spiral shell architecture for the development of the proposed cellular airfoil.

Furthermore, studies on integrated shell–lattice structures have demonstrated that the interaction between an external skin and the internal cellular network plays an important role in load transfer and the resulting mechanical response [18]. These findings highlight the potential of internally architected structures for tailoring the structural behavior of aerodynamic components without modifying their external profiles.

Despite these advances, most investigations of cellular aerospace structures have focused on conventional periodic lattices, including repeated unit-cell architectures and optimized lattice infills [1, 16]. In parallel, bio-inspired architected materials have predominantly been investigated in the context of energy absorption, impact resistance, and generic cellular structures [4–7]. Comparatively limited attention has been devoted to the integration of non-periodic, nested cellular architectures derived from natural hierarchical patterns into airfoil structures. In particular, the combined abstraction of plant-based cellular organization and spiral shell geometry for generating a parametrically controlled internal airfoil architecture has not been systematically investigated. Moreover, the influence of the relative position and scaling of nested internal profiles on bending stiffness, stress redistribution, and the onset of local yielding remains insufficiently understood.

Therefore, the present study proposes a bio-inspired cellular airfoil architecture based on the geometric abstraction of the hierarchical cellular organization of the banana pseudostem and the progressive arrangement associated with spiral shell structures. The proposed architecture is integrated into NACA0010 and NACA2412 airfoil profiles and systematically controlled using two geometric parameters: the position factor K_1 and scaling factor K_2. Eighteen configurations are generated and evaluated through finite element analysis to investigate their load–displacement response, bending stiffness, von Mises stress distribution, and first-yield load. The structures are designed with potential SLM-based fabrication in mind, providing a route toward geometrically complex metallic cellular airfoils. The objective is to identify the relationship between internal cellular geometry and structural response and to establish design guidelines for balancing global stiffness, local stress concentration, and load-carrying capacity in bio-inspired cellular airfoil structures.

2. Materials and methods

2.1. Bio-inspired cellular airfoil design

Inspired by the efficient load-bearing characteristics of natural cellular structures, a bio-inspired internal architecture was developed and integrated into NACA airfoils. Rather than directly replicating biological geometries, the proposed design adopts the structural principles observed in the cross-section of banana stems and spiral shells, including hierarchical organization, continuous load paths, and gradual variation of cell dimensions. These features contribute to an efficient distribution of stresses while reducing structural weight.

As illustrated in Fig. 2, the proposed architecture consists of three nested airfoil profiles interconnected by transverse members, forming a non-periodic bio-inspired cellular framework. Unlike conventional lattice structures composed of repeating unit cells, the present architecture follows the geometry of the airfoil itself while maintaining continuous load-transfer paths throughout the structure.

The internal structure was designed to provide a higher cell density in the forward region of the airfoil. In contrast, progressively larger cells were introduced toward the trailing edge to reduce material usage and maintain continuous load-transfer paths. The resulting architecture forms a lightweight structural framework developed as a conceptual

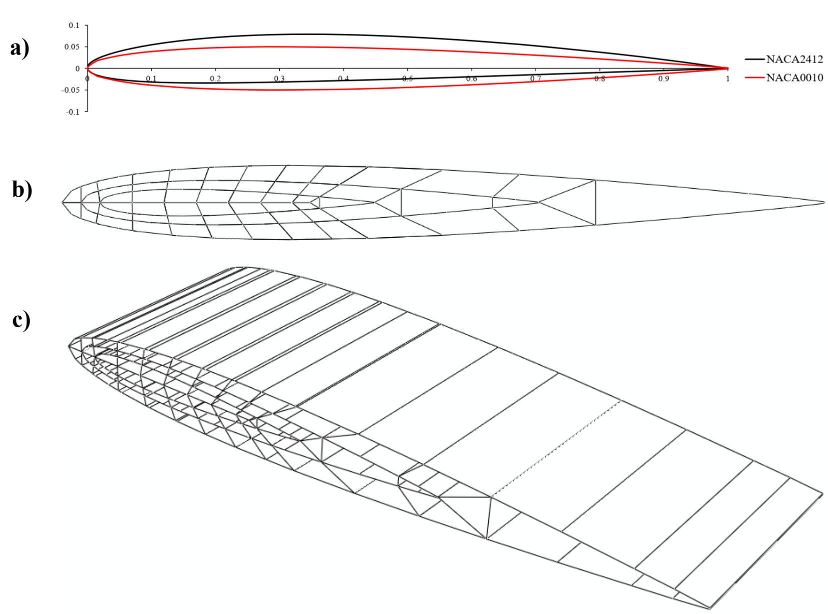

Fig. 2. Design procedure of the proposed bio-inspired cellular airfoil. a) Selected NACA airfoil profiles, b) construction of the nested guide airfoils for defining the internal cellular architecture, and c) final three-dimensional bio-inspired cellular airfoil model.

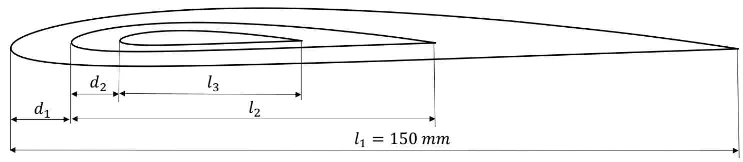

Fig. 3. Definition of the geometric parameters used for the generation of the bio-inspired cellular airfoil, illustrating the nested airfoil profiles, chord lengths (l_1, l_2, and l_3), offset distances (d_1 and d_2), and the parametric definitions of K_1 and K_2.

design for future fabrication using selective laser melting (SLM). To investigate the influence of the internal architecture on the structural behavior of the airfoil, the cellular geometry was parameterized using a set of geometric variables. The parameterization procedure and the investigated design configurations are presented in the following section.

2.2. Parametric geometry generation

The proposed bio-inspired cellular architecture was generated using a parametric design methodology in which the internal guide airfoils were defined through a small number of geometric parameters while preserving the external airfoil profile. As illustrated in Fig. 3, the cellular architecture was constructed from three nested airfoils with progressively smaller chord lengths. The outer profile (l_1) defines the aerodynamic boundary of the airfoil, whereas the two inner profiles (l_2 and l_3) determine the internal cellular framework.

The geometry of the nested airfoils is governed by two dimensionless parameters and one dimensional parameter. The scaling factor K_2 controls the relative size of successive nested airfoils and is defined as $K_2=l_2/l_1= l_3/l_2$. Ensuring that the inner profiles are generated by a constant scaling ratio. The position factor K_1 controls the relative spacing between successive airfoils and is expressed as $K_1=d_2/d_1$. Where d_1 is the offset distance between the first and second airfoils, and d_2 is the offset distance between the second and third airfoils. In this study, d_1 is denoted by d and represents the primary offset parameter. By varying K_1 and K_2 while maintaining the external airfoil geometry, different internal cellular architectures were generated automatically using a MATLAB algorithm. Two reference airfoil profiles, NACA0010 and NACA2412, were considered. For each profile, three values of K_1 (1.00, 0.75, and 0.50) were combined with three values of K_2 (0.70, 0.60, and 0.50), resulting in nine configurations per airfoil and a total of eighteen parametric models. The offset distance d was fixed for each airfoil family to preserve geometric consistency.

Table 1. Geometric parameters used in the parametric generation of the bio-inspired cellular airfoils.

Symbol	Definition	Values
l_1	Chord length of the outer airfoil	150 mm
l_2	Chord length of the second airfoil	K_2l_1
l_3	Chord length of the third airfoil	K_2l_2
$d=d_1$	Leading-edge offset distance between the first and second airfoils	37.5 mm (NACA0010), 15 mm (NACA2412)
d_2	Offset distance between the second and third airfoils	K_1d
K_1	Position factor d_2/d_1	1.00, 0.75, 0.50
K_2	Scaling factor $l_2/l_1=l_3/l_2$	0.70, 0.60, 0.50
D_s	Spanwise depth	50 mm

2.3. Material selection and SLM considerations

AlSi10Mg was selected for the finite element analysis because of its widespread application in selective laser melting (SLM) for lightweight aerospace structures. The material was modeled using an elastic–perfectly plastic constitutive law, in which the elastic response was defined by Young's modulus and Poisson's ratio, while yielding was introduced using the specified yield strength without strain hardening. Identical material properties were assigned to all airfoil configurations to ensure that the observed differences in structural performance resulted solely from variations in the bio-inspired cellular geometry. The mechanical properties used in the numerical simulations are summarized in Table 2.

Although an elastic–perfectly plastic material model was adopted, the prescribed loading level was selected such that the overall structural response remained predominantly elastic. Localized yielding was initiated only in a limited number of configurations and remained confined to small regions near stress concentrations, without causing significant plastic redistribution or affecting the global load–displacement response.

The present study focuses on the structural design and numerical evaluation of the proposed bio-inspired cellular architecture. Practical fabrication of enclosed cellular airfoils by SLM would require additional manufacturing considerations, including build orientation, powder evacuation, and support accessibility. In practical applications, powder removal could be facilitated by incorporating discrete powder evacuation holes or drainage channels within the airfoil, or by manufacturing the airfoil as multiple sections followed by post-build joining. These manufacturing-related aspects were beyond the scope of the present structural investigation and will be addressed in future work.

Table 2. Mechanical properties of AlSi10Mg used in the finite element analysis.

Property	Symbol	Value
Density	ρ	2670 kg/m³
Young's modulus	E	69 GPa
Poisson's ratio	ν	0.30
Yield strength	σ_y	230 MPa
Ultimate tensile strength	σ_u	360 MPa

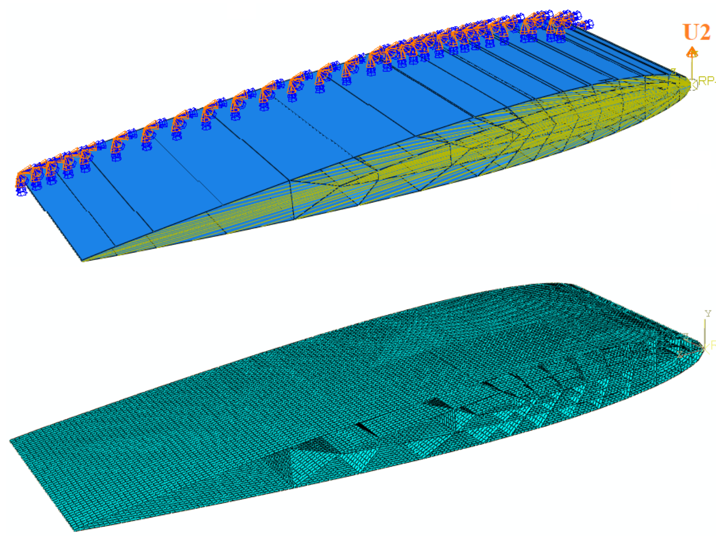

Fig. 4. Finite element model and boundary conditions.

2.4. Finite element model

The structural performance of the proposed bio-inspired cellular airfoils was evaluated using ABAQUS/Standard. The two-dimensional cellular airfoil geometries were extruded to generate three-dimensional shell models with a spanwise depth of 50 mm. All structural components, including the outer skin and internal cellular members, were assigned a uniform thickness of 4 mm and the material properties listed in Table 2.

The numerical model was discretized using S4R shell elements, i.e., four-node doubly curved shell elements with reduced integration, hourglass control, and finite membrane strains. An element size of 1 mm was adopted throughout the model to accurately capture the complex cellular architecture while maintaining computational efficiency. As illustrated in Fig. 4, the root cross-section of the airfoil was fully constrained, whereas a prescribed vertical displacement of 0.25 mm was applied to a reference point rigidly coupled to the opposite cross-section, producing a bending deformation of the structure. The same loading and boundary conditions were applied to all configurations to ensure a consistent comparison of their structural responses.

The loading end of the airfoil remained geometrically open. To ensure a uniform transfer of the prescribed displacement, all nodes located on the end cross-section, including the outer skin and the internal cellular members, were rigidly coupled to a reference point, at which the displacement boundary condition was applied.

3. Results and discussion

This section presents the finite element analysis results of the bio-inspired cellular airfoils. The structural response of the eighteen parametric configurations was evaluated under identical loading and boundary conditions. The influence of the airfoil profile (NACA0010 and NACA2412), together with the geometric parameters K_1 and K_2, was investigated by comparing the von Mises stress distribution, displacement field, and overall structural behavior. The results are presented and discussed in the following sections.

3.1. Load–displacement response and bending stiffness

Fig. 5 presents the load–displacement responses of the bio-inspired cellular configurations based on the NACA0010 and NACA2412 profiles. All models exhibit an approximately linear load–displacement response over the investigated displacement range. This behavior indicates that the global stiffness response remains predominantly elastic, although localized yielding may occur in highly stressed regions according to the elastic–perfectly plastic material model. The slope of each curve represents the global bending stiffness of the corresponding cellular airfoil and was calculated as the ratio of the reaction load to the prescribed displacement. The resulting stiffness values for different combinations of K_1 and K_2 are summarized in Table 3.

A clear difference is observed between the two airfoil families. The NACA0010 configurations exhibit bending stiffness values ranging from 41.17 to 47.97 kN/mm, whereas substantially higher values of 84.30–99.90 kN/mm are obtained for the NACA2412 models. Thus, depending on the cellular configuration, the NACA2412 profile provides approximately three to two times the bending stiffness of the corresponding NACA0010 airfoil.

The influence of the geometric parameters is particularly evident for the NACA2412 configurations. For all investigated values of K_2, decreasing K_1 from 1.0 to 0.5 progressively increases the bending stiffness. The maximum stiffness of 99.90 kN/mm is obtained at K_1=0.5 and K_2=0.5, representing an increase of approximately 18.5% compared with the corresponding K_1=1.0 configuration. Similarly, reducing K_2 generally increases the stiffness, with the most pronounced improvement observed at K_1=0.5.

In contrast, the NACA0010 configurations exhibit a less uniform parametric trend. Although the highest stiffness of 47.97 kN/mm is also obtained at K_1=0.5 and K_2=0.5, the effects of K_1 and K_2 are dependent on their specific combination. This behavior indicates an interaction between the position and scaling parameters in controlling the load-

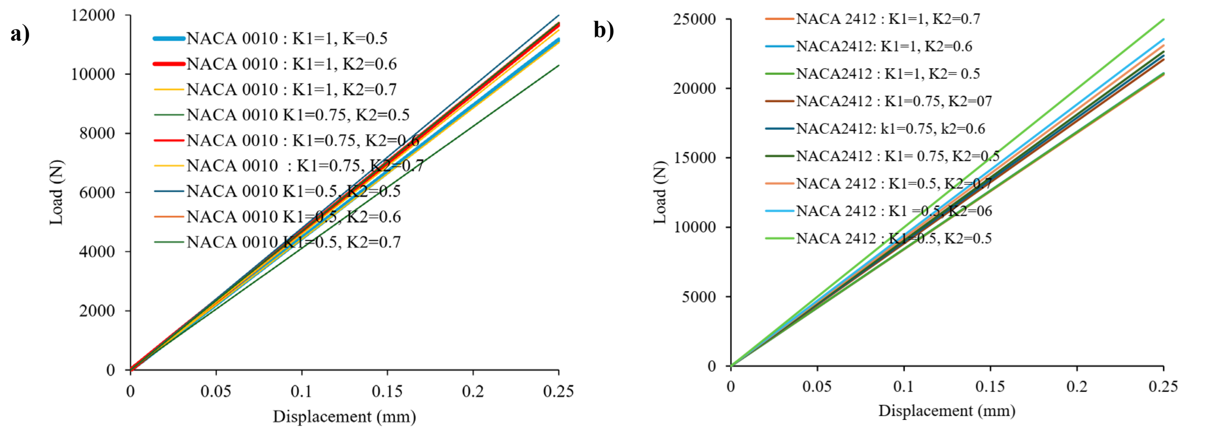

Fig. 5. Load–displacement responses of the bio-inspired cellular airfoils with different values of K_1 and K_2: a) NACA0010 and b) NACA2412.

transfer paths within the symmetric cellular airfoil. Overall, the results demonstrate that the structural response is governed by both the external airfoil geometry and the arrangement of the internal cellular network.

3.2. Stress distribution and effect of geometric parameters

Figs. 6 and 7 compare the von Mises stress distributions of elected NACA0010 and NACA2412 configurations, respectively. The selected models enable the independent effects of K_1 and K_2 to be evaluated by varying one geometric parameter while maintaining the other constant. For all configurations, elevated stresses are primarily observed near the fixed root and at the connections between the outer skin and internal cellular members. These regions represent the primary load-transfer zones under bending and are therefore more susceptible to local stress concentrations.

The effect of K_1 is clearly non-monotonic. For the NACA0010 airfoil at K_2=0.6, the maximum von Mises stress decreases from 202.4 MPa at K_1= 1.0 to 145.3 MPa at K_1= 0.75, but subsequently increases to 269.3 MPa when K_1 is reduced to 0.5. A similar trend is observed for the NACA2412 profile, for which the corresponding peak stresses are 330.7, 289.4, and 305.8 MPa, respectively. These results indicate that reducing the spacing between the nested airfoils does not continuously improve the stress response. Instead, the intermediate value of K_1=0.75 provides a more favorable arrangement of the internal load-transfer paths and limits localized stress amplification.

A more consistent trend is observed for K_2. At K_1=0.75, decreasing K_2 from 0.7 to 0.5 reduces the maximum von Mises stress from 229.1 to 136.1 MPa for the NACA0010 airfoil. Similarly, the peak stress in the NACA2412 configurations decreases from 305.3 to 276.7 MPa. The denser cellular architecture generated at lower K_2 values provides additional structural connections and promotes a more effective redistribution of the bending load through the internal network.

The stress contours further show that the symmetric NACA0010 profile develops a comparatively more regular stress field, whereas the cambered geometry of the NACA2412 airfoil produces a more asymmetric stress distribution. Nevertheless, the parametric trends remain similar for both profiles. In particular, the intermediate position factor K_1=0.75, combined with the lower scaling factor K_2=0.5, provides the most favorable stress response among the compared configurations. These observations confirm that the relative arrangement of the nested airfoils is as important as the cellular density in controlling local stress concentrations.

Table 3. Bending stiffness of the NACA0010 and NACA2412 bio-inspired cellular airfoils for different combinations of K_1 and K_2.

	NACA0010		
	K_1=0.5	**K_1=0.75**	**K_1=1**
K_2=0.5	47.97	41.17	44.64
K_2=0.6	46.97	46.53	46.73
K_2=0.7	46.92	45.95	44.25
	NACA2412		
K_2=0.5	99.90	90.61	84.30
K_2=0.6	94.21	89.46	84.39
K_2=0.7	92.4	88.34	83.99

3.3. Integrated structural performance and design selection

Table 4 provides an integrated comparison of the eighteen bio-inspired cellular airfoil configurations in terms of reaction load, bending stiffness, maximum von Mises stress, and estimated first-yield load. The first-yield load was estimated by scaling the reaction load according to the ratio of the material yield strength to the maximum von Mises stress. This value corresponds to the estimated load level at which the most critically stressed region first reaches the yield strength, marking the onset of localized plastic deformation. Although subsequent yielding is governed by the elastic–perfectly plastic material model adopted in the finite element analysis, the estimated first-yield load provides a comparative measure of the load capacity of each configuration before local yielding.

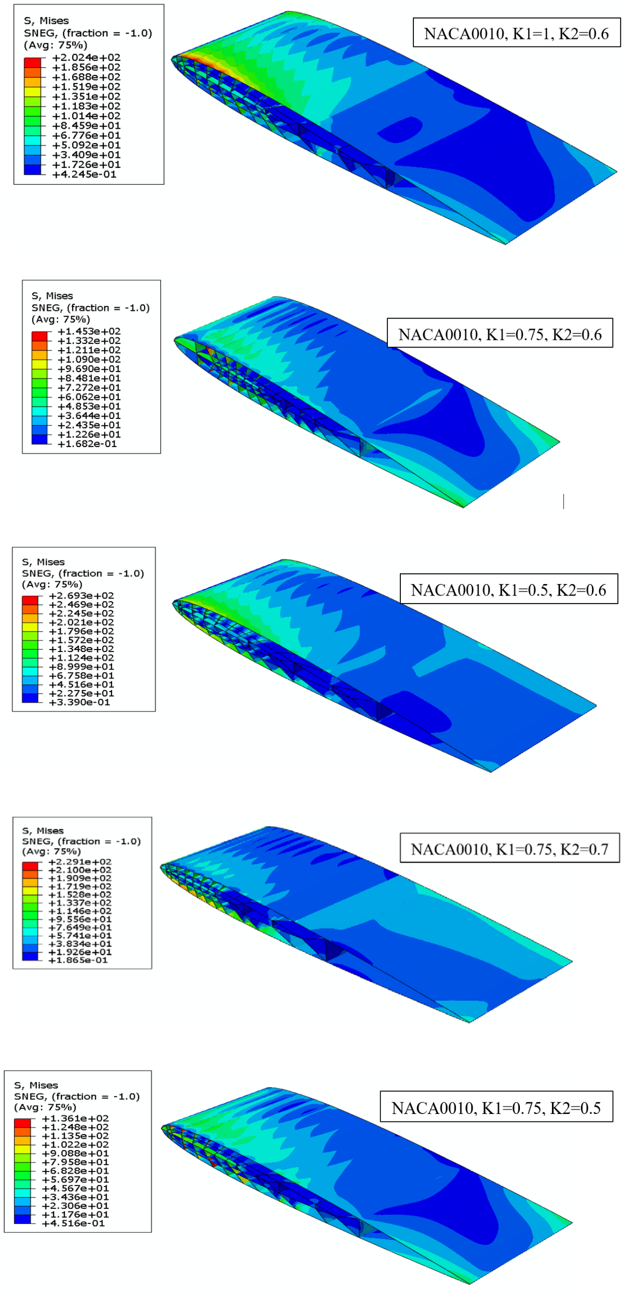

Fig. 6. Von Mises stress distributions of selected NACA0010 cellular airfoils illustrating the effects of K_1 and K_2 on the internal stress field.

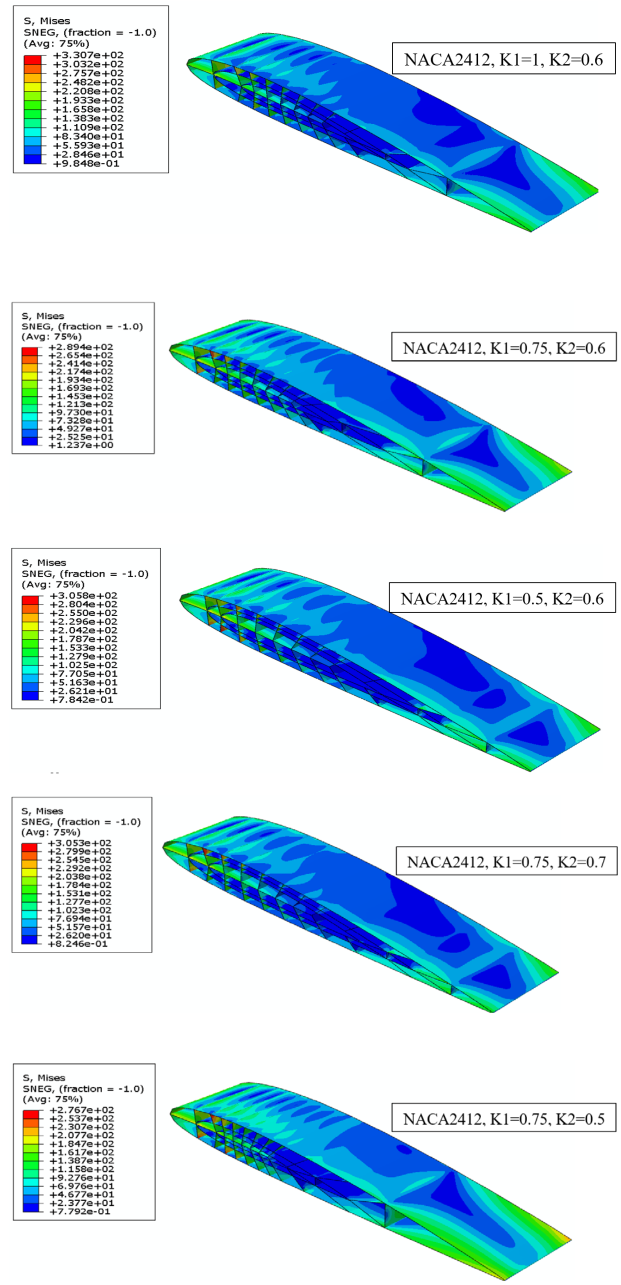

Fig. 7. Von Mises stress distributions of selected NACA2412 cellular airfoils illustrating the effects of K_1 and K_2 on the internal stress field.

The results reveal a clear trade-off between structural stiffness and local stress concentration. The NACA2412 configuration with K_1=0.5 and K_2=0.5 exhibits the highest bending stiffness (99.9 kN/mm); however, the stress contours indicate pronounced local stress concentrations, demonstrating that the stiffest configuration does not necessarily provide the most favorable stress response. In contrast, the configuration with K_1=0.75 and K_2=0.5 combines a high bending stiffness of 90.6 kN/mm with the lowest peak stress within the NACA2412 series (276.7 MPa), leading to the highest estimated first-yield load of 18.8 kN. Therefore, this configuration provides the most favorable balance between stiffness and load-carrying capacity among the investigated designs.

These findings demonstrate that maximum stiffness alone is not an adequate criterion for selecting the optimum cellular architecture. Instead, the combined evaluation of global stiffness and local stress response provides a more meaningful basis for comparing and selecting bio-inspired cellular airfoil configurations.

Table 4. Structural performance of the parametric bio-inspired cellular airfoil configurations with different values of K_1 and K_2.

K_1	K_2	Load at 0.25 mm (N)	Stiffness (kN/mm)	σ max (MPa)	First-yield load (N)
		NACA 0010			
1	0.7	11060	44.3	149.8	16,985
1	0.6	11680	46.7	202.4	13,276
1	0.5	11160	44.6	143.5	17,886
0.75	0.7	11490	46.0	229.1	11,533
0.75	0.6	11630	46.5	145.3	18,414
0.75	0.5	10300	41.2	136.1	17,395
0.5	0.7	11730	46.9	215.5	12,519
0.5	0.6	11740	47.0	269.3	10,029
0.5	0.5	12000	48.0	167.3	16,485
		NACA 2412			
1	0.7	21000	84.0	290.1	16650
1	0.6	21100	85.2	330.7	14670
1	0.5	21070	84.3	360.0	13460
0.75	0.7	22090	88.3	305.3	16640
0.75	0.6	22370	89.5	289.4	17780
0.75	0.5	22650	90.6	276.7	18830
0.5	0.7	23100	92.4	360.0	14760
0.5	0.6	23550	94.2	305.8	17710
0.5	0.5	24980	99.9	360.0	15960

4. Conclusions

This study presented a parametric finite element investigation of bio-inspired cellular airfoils designed for potential fabrication using selective laser melting (SLM). The proposed internal architecture, inspired by the hierarchical characteristics of natural structures, was integrated into NACA0010 and NACA2412 profiles. Eighteen configurations were generated by systematically varying the position factor (K_1) and scaling factor (K_2) to evaluate their effects on bending stiffness, stress distribution, and load-carrying capacity.

The results demonstrated that both the external airfoil profile and the internal cellular architecture significantly influence the structural response. The NACA2412 configurations exhibited bending stiffness values between 84.0 and 99.9 kN/mm, approximately twice those obtained for the NACA0010 configurations. The geometric parameters also altered the internal load-transfer paths and local stress concentrations, with the effects being particularly pronounced for the cambered NACA2412 profile.

Among the investigated designs, the NACA2412 configuration with K_1=0.5 and K_2=0.5 exhibited the highest bending stiffness of 99.9 kN/mm. However, the development of higher local stresses demonstrated that maximum stiffness alone is insufficient for selecting the optimum cellular architecture. The NACA2412 configuration with K_1=0.75 and K_2=0.5 provided the most balanced structural response, combining a bending stiffness of 90.6 kN/mm with a maximum von Mises stress of 276.7 MPa and the highest estimated first-yield load of 18.8 kN.

Overall, the findings demonstrate that controlled variation of the internal cellular geometry can provide an effective means of tailoring the structural response of airfoil structures without modifying their external aerodynamic profiles. The proposed parametric design approach offers a promising framework for the development of structurally efficient bio-inspired airfoils with complex internal architectures suitable for SLM-based manufacturing. Future work should focus on experimental fabrication and mechanical testing of the selected configurations, together with the investigation of SLM-induced defects, surface roughness, residual stresses, and manufacturing constraints to validate the numerical findings and assess their practical applicability.

CRediT authorship contribution statement

Ata Khabaz-Aghdam: Conceptualization, Methodology, Formal Analysis, Validation, Writing – original draft, Writing – review & editing, Supervision, Project Administration.
Elisee Abu Mulamba Tshibeng: Investigation, Software, Data Curation, Visualization.
Omar Wambele Nsimba: Investigation, Software, Data curation, Visualization.

Data availability

The data underlying this article will be shared on reasonable request to the corresponding author.

Declaration of competing interest

The authors declare no competing interests.

Funding and acknowledgment

The authors acknowledge the Department of Aeronautical Engineering, Faculty of Aviation and Space Sciences, University of Kyrenia, for providing the academic and computational environment supporting this study.

References

[1] N. Khan, A. Riccio, A systematic review of design for additive manufacturing of aerospace lattice structures: Current trends and future directions, Prog. Aerosp. Sci. 149 (2024) 101021. https://doi.org/10.1016/j.paerosci.2024.101021.
[2] M. Benedetti, A. du Plessis, R.O. Ritchie, M. Dallago, N. Razavi, F. Berto, Architected cellular materials: A review on their mechanical properties towards fatigue-tolerant design and fabrication, Mater. Sci. Eng. R: Rep. 144 (2021) 100606. https://doi.org/10.1016/j.mser.2021.100606.
[3] Z. Alomar, F. Concli, A review of the selective laser melting lattice structures and their numerical models, Adv. Eng. Mater. 22 (2020) 2000611. https://doi.org/10.1002/adem.202000611.
[4] A. du Plessis, C. Broeckhoven, I. Yadroitsava, I. Yadroitsev, C.H. Hands, et al., Beautiful and functional: A review of biomimetic design in additive manufacturing, Addit. Manuf. 27 (2019) 408–427. https://doi.org/10.1016/j.addma.2019.03.033.

[5] S.H. Siddique, P.J. Hazell, H. Wang, J.P. Escobedo, A.A.H. Ameri, Lessons from nature: 3D printed bio-inspired porous structures for impact energy absorption – A review, Addit. Manuf. 58 (2022) 103051. https://doi.org/10.1016/j.addma.2022.103051.

[6] M.I. Chibinyani, T.C. Dzogbewu, M. Maringa, A. Muiruri, Natural cellular structures in engineering designs built via additive manufacturing, Mater. Technol. 40 (2025) 2443211. https://doi.org/10.1080/10667857.2024.2443211.

[7] A.S. Mirhakimi, D. Dubey, M.A. Elbestawi, Laser powder bed fusion of bio-inspired metamaterials for energy absorption applications: A review, J. Mater. Res. Technol. 31 (2024) 2126–2155. https://doi.org/10.1016/j.jmrt.2024.06.234.

[8] A.N. Saputro, M.S. Anrokhi, A. Muhyi, M.F. Arif, Mechanical behavior of 3D-printed banana pseudostem-like structure, IOP Conf. Ser. Earth Environ. Sci. 830 (2021) 012072. https://doi.org/10.1088/1755-1315/830/1/012072.

[9] D.A. Chen, B.E. Ross, L.E. Klotz, Parametric analysis of a spiraled shell: Learning from nature's adaptable structures, Designs. 2 (2018) 46. https://doi.org/10.3390/designs2040046.

[10] G. Chouhan, B.M. Gunji, P. Bidare, D. Ramakrishna, R. Kumar, Experimental and numerical investigation of 3D printed bio-inspired lattice structures for mechanical behaviour under quasi-static loading conditions, Mater. Today Commun. 35 (2023) 105658. https://doi.org/10.1016/j.mtcomm.2023.105658.

[11] Z.H. Li, Y.F. Nie, B. Liu, Z.Z. Kuai, M. Zhao, F. Liu, Mechanical properties of AlSi10Mg lattice structures fabricated by selective laser melting, Mater. Des. 192 (2020) 108709. https://doi.org/10.1016/j.matdes.2020.108709.

[12] X. Han, H. Zhu, X. Nie, G. Wang, X. Zeng, Investigation on selective laser melting AlSi10Mg cellular lattice strut: Molten pool morphology, surface roughness and dimensional accuracy, Materials. 11 (2018) 392. https://doi.org/10.3390/ma11030392.

[13] E. Ossola, A.A. Shapiro, A. Pate, S. Firdosy, E. Brusa, R. Sesana, Fabrication defects and limitations of AlSi10Mg lattice structures manufactured by selective laser melting, Proc. Inst. Mech. Eng. L: J. Mater. Des. Appl. 235 (2021) 2071–2082. https://doi.org/10.1177/14644207211012726.

[14] H.R. Kotadia, G. Gibbons, A. Das, P.D. Howes, A review of laser powder bed fusion additive manufacturing of aluminium alloys: Microstructure and properties, Addit. Manuf. 46 (2021) 102155. https://doi.org/10.1016/j.addma.2021.102155.

[15] L. Zhao, L. Song, J.G. Santos Macías, Y. Zhu, M. Huang, et al., Review on the correlation between microstructure and mechanical performance for laser powder bed fusion AlSi10Mg, Addit. Manuf. 56 (2022) 102914. https://doi.org/10.1016/j.addma.2022.102914.

[16] N. Khan, V. Acanfora, A. Riccio, Non-conventional wing structure design with lattice infilled through design for additive manufacturing, Materials. 17 (2024) 1470. https://doi.org/10.3390/ma17071470.

[17] T. Al-Oussainne, A. Khabaz-Aghdam, Finite element analysis of additive manufacturing-enabled cellular architectures for morphing airfoil applications, Synth. Sinter. 6 (2026) 41–48. https://doi.org/10.53063/synsint.2026.61323.

[18] Y. Bai, J. Gao, C. Huang, Y. Li, Mechanical properties and energy absorption of integrated AlSi10Mg shell structures with BCC lattice infill, Chin. J. Mech. Eng. 36 (2023) 143. https://doi.org/10.1186/s10033-023-00973-8.